Organic Polymer Analysis by Laser Ionization Mass Spectrometry and Pattern Recognition Techniques

FILIPPO RADICATI DI BROZOLO and ROBERT W. ODOM, *Charles Evans & Associates, 301 Chesapeake Drive, Redwood City, California 94063,* and PETER DE B. HARRINGTON and KENT J. VOORHEES, *Department of Chemistry and Geochemistry, Colorado School of Mines, Golden, Colorado 80401*

Synopsis

Results obtained by combining pattern recognition techniques with the organic microanalysis capability of laser ionization mass spectrometry (LIMS) for identifying and classifying the mass spectra produced from 19 different polymer formulations are reported. The data demonstrates that the LIMS mass spectra of many polymers are sufficiently unique to permit accurate classification of different polymers. The results obtained also suggest that pattern recognition procedures combined with laser microprobe analyses could provide a routine and reliable method of performing microanalytical characterization of unknown polymers.

INTRODUCTION

Laser ionization mass spectrometry (LIMS) employs a high power density (irradiance), focused laser pulse to vaporize and ionize the constituents of solid sample materials.[1] The LIMS technique is also referred to as laser microprobe mass spectrometry and is designated by acronyms such as LAMMS and LAMMA. Pulsed laser ionization coupled with time-of-flight mass spectrometry (TOFMS) provides a microanalysis capability in which essentially all the different mass ions produced from a single analysis area can be detected for each laser pulse.[2] Typical performance characteristics of state-of-the-art LIMS instrumentation include elemental detection sensitivities from 0.1 to 100 part per million atomic (ppma) and mass detection ranges as high as 1000 atomic mass units (amu) within analytical areas 1–5 μm in diameter.[3] These unique microanalysis capabilities have been applied to a wide variety of elemental microanalyses.[4] Researchers employing laser microprobe mass spectrometry have long recognized that the technique has the potential for providing sensitive organic or molecular microanalysis of a variety of material surfaces.[5] As a consequence, the interest is increasing in the organic microanalysis capability of LIMS for polymers[6] and organic compounds.[7]

The objectives of the work were to determine how well the LIMS technique could produce characteristic mass spectra from different organic polymer formulations and how useful these mass spectra are for identifying an unknown polymer. Principal component/discriminant analysis and expert system techniques were applied to LIMS data sets that contained spectra of as many as

Journal of Applied Polymer Science, Vol. 41, 1737–1752 (1990)
 CCC 0021-8995/90/7-81737-16$04.00

19 different organic polymers.[8,9] The results described demonstrate that LIMS mass spectra of different polymers are often quite distinct and can be readily resolved using pattern recognition techniques. In fact, this data illustrates that different types of polymers having similar chemical structures can be readily separated based on their characteristic LIMS mass spectra.

EXPERIMENT

Samples

Table I lists the various polymers analyzed along with a description of their physical form. The polymers were either thin films (1 μm thick) or bulk solids. The thin-film samples were prepared by embedding beads or powders of the samples into Spurrs epoxy resin and microtoming thin sections that were mounted onto Si substrates. The locations of the embedded polymers were readily apparent in the optical microscope of the laser microprobe, which allowed acquisition of mass spectra from the embedded polymer and not the Spurrs epoxy. Thin sections of pure Spurrs were also analyzed in this evaluation. The bulk (thick) samples were prepared by cutting out a section of the sample or by scraping away the top 1 mm of sample surface. Cleaned surgical knives were used to avoid contaminating the sample surfaces. The preparation of thin sections as well as the cutting or scraping of the top layers of the bulk specimens minimized the ion signals produced by chemicals such as mold release compounds and atmospheric contaminants.

TABLE I
Organic Polymers Analyzed by LIMS

Polymer	Physical form
1. Nylon 6	TF[a]
2. Nylon 12	TF
3. Poly(1,4-butylene) terephthalate	TF
4. Polycarbonate	TF
5. Polystyrene	TF
6. Spurrs epoxy	TF
7. Mylar 500D poly(ethylene) terephthalate	TF
8. Polyimide S-11 (DuPont 1556)	TF
9. Polyimide S-09 (GE SPI 115)	TF
10. Polyimide S-24 (Hitachi PIX-1400)	TF
11. Polyimide S-10 (Toray LP-64)	TF
12. Polyimide S-19 (Ciba Geigy Probimide 284)	TF
13. Photoresist 1400-33 (Shipley)	TF
14. 59301 Epoxy (DDS/TGDDM, 0.2)	BS[b]
15. 59304 Epoxy (DDS/TGDDM, 0.75)	BS
16. 59306 Epoxy (DDS/TGDDM, 1.0)	BS
17. 59307 Epoxy (DDS/TGDDM, 1.5)	BS
18. Production Epoxy	BS
19. Texin 455D, Polyurethane (Mobay)	BS

[a] TF designates thin film.
[b] BS designates bulk solid.

LIMS Analysis

The LIMS analyses were performed on a Cambridge Mass Spectrometry, Ltd. (Cambridge, England) Model LIMA 2A reflection mode laser microprobe instrument, which has been described in detail elsewhere.[9] Fifteen positive and negative ion laser microprobe mass spectra were obtained at 3 different laser irradiances from the 19 polymers listed in Table I. The laser irradiances corresponded to the threshold for ionization and irradiance values, which produced 5 and 25 times the threshold ion intensity. Over 1100 mass spectra were acquired from this polymer set. Mass spectra were typically acquired over a mass range from 0 to 300 amu. The upper mass range was limited by the Sony-Tektronix 390 AD transient recorder that operated at a sampling frequency of 60 MHz. Essentially no ions were detected above mass 300 with the LIMS configuration used in this study.

Data Analysis

The spectra were normalized to correct for differences in concentrations and ionization yields. The mass spectra were normalized to unit vector length autoscaled so that peaks of higher masses and lower abundances were weighted equally with peaks of lower mass and higher abundance. The resulting data sets were compressed by eigenvector transformations so that the data would be overdetermined by a factor of 3. These eigenvectors also represented at least 80% of the variance of the data set. Sample distributions were converted from a multidimensional space to a two-dimensional space by plotting the sample scores on two principal components at a time (Karhunen-Loeve plots). The classification algorithms used the principal component scores as variables.

The LIMS data was also analyzed using a traditional discriminant analysis approach and an expert system that performs classification via an entropy calculation. The expert system converts the scores from the principal components into a symbolic representation using a modified ID3 algorithm.[11] Because the categories in the principal component training set are known, an attribute can be found that separates the categories. The median value of two adjacent scores from different categories is used as the attribute. The attribute with the lowest entropy is selected in the rule-building system that partitions the data.

The entropy of classification for class C with attribute A, $H(C|A)$, is a measure of the uncertainty after a classification is made according to a decision criterion. The entropy of classification is given by

$$H(C|a_j) = -\sum_{i=1}^{n} p(c_i|a_j) \ln p(c_i|a_j) \tag{1}$$

$$H(C|A) = \sum_{j=1}^{m} p(a_j) H(C|a_j) \tag{2}$$

Equation (1) gives the entropy for an attribute where n is the number of different classes and $p(c_i|a_j)$ is a probability obtained by counting the number of observations of class i with attribute j and dividing that number by the number of occurrences of the jth attribute. Equation (2) is the sum of the entropy for

each attribute weighted by the prior probability the attribute occurs. The number of attributes is m and $p(a_j)$ is a probability obtained by counting the number of observations with a given attribute and dividing that number by the total number of observations. A zero entropy will be obtained when all the samples in the training set are correctly classified.

Cross validation of the results was used to evaluate the performance of the expert system and discriminant analysis. For example, cross validation of the canonical variates provides an unbiased measure of the predictive ability of the different canonical variates for classifying the different spectra into the correct category. Cross validation is accomplished by removing a spectrum from the training set, building a model based on the canonical variates, and then determining how well the model predicts the category of the spectrum that was removed. All calculations were performed on an IBM PS/2 Model 60 computer operating under MS-DOS 3.3. All computations were performed by the RESOLVE software package, which is a general-purpose data analysis system.[12] All graphs were obtained from screen dumps of the RESOLVE software to a Hewlett-Packard Laser Jet 500+ printer.

RESULTS AND DISCUSSION

Polymers 1 through 5, 6, and 19 in Table I are relatively common polymers employed in a variety of applications. The polyimide and photoresist samples are routinely used in the microelectronics industry. The DDS/TGDDM epoxy material is used as the binder matrix for continuous carbon fiber reinforced composites.[13] Polymers 1–5 and 7 have relatively simple structures while many of the other polymers are chemically complex. For example, the DDS/TGDDM material is a mixture of a few parts per hundred amine function of 4,4′-diaminodiphenyl sulfone (DDS) with 80–90% by weight of tetraglycidyl 4,4′-diamino diphenylmethane (TGDDM) and 10–20% of a polyglycidyl ether of bisphenol A Novolac epoxy. The various DDS/TGDDM epoxies analyzed contained different hardener (DDS) to resin (TGDDM) ratios. One of the objectives of this study was to determine whether the LIMS mass spectra would provide distinct characterizations of the different epoxy formulations.

Representative laser microprobe mass spectra of several of these polymers are illustrated in Figures 1 through 4. It should be noted that the ordinate of the spectra is a logarithmic scale. This representation presents the false impression that there are numerous peaks in the spectra, while in fact, only a small number of the more intense peaks are present when projected on a linear scale. The more intense peaks are numbered in the figures. High irradiance positive ion spectra of nylon 12 and Mylar 500D are illustrated in Figure 1. The spectra are comprised primarily of $X_xH_y^+$ cluster ions. The Mylar mass spectrum extends to higher mass values and contains obvious aromatic peaks at masses 77, 91, and 105. The peaks at m/z 149 and 165 are probably formed from the terephthalate species.[14] Figure 2 illustrates low-irradiance mass spectra produced from the polyurethane and one of the DDS/TGDDM formulations. These spectra contain $C_xH_y^+$ cluster ions, several aromatic ions along with distinctive higher mass peaks. Figure 3 shows low-irradiance, positive ion mass

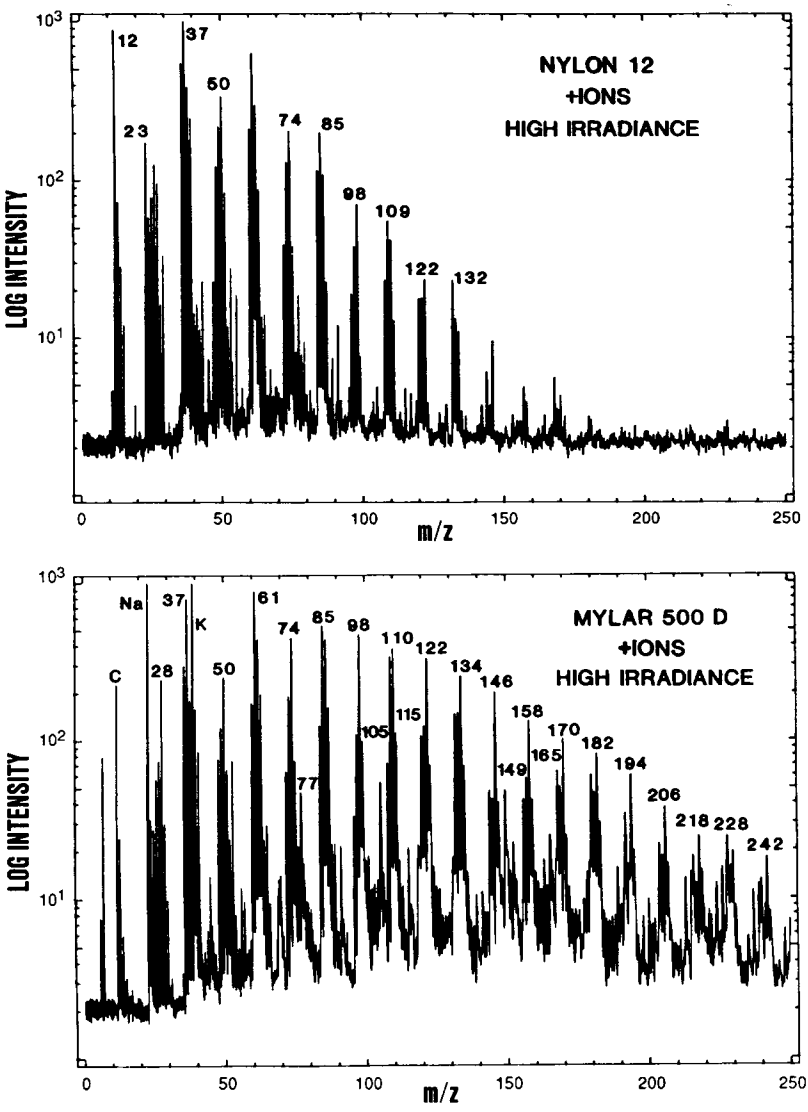

Fig. 1. High laser irradiance, positive ion LIMS mass spectra of nylon 12 and Mylar 500D.

spectra of two of the DDS/TGDDM samples. The low-irradiance analysis of these samples provided the most distinctive and reproducible mass spectra (see following discussion). The top spectrum has a detector baseline shift that is indicative of a high level of ionization and/or metastable decompositions in the mass spectrum. These samples were bulk specimens having a greenish-red color and appeared to absorb the incident laser light quite efficiently. Efficient absorption could account for the observed high degree of ionization. The spectra contain the familiar $C_xH_y^+$ cluster ions along with several aromatic ion signals. These two spectra do, however, appear qualitatively different.

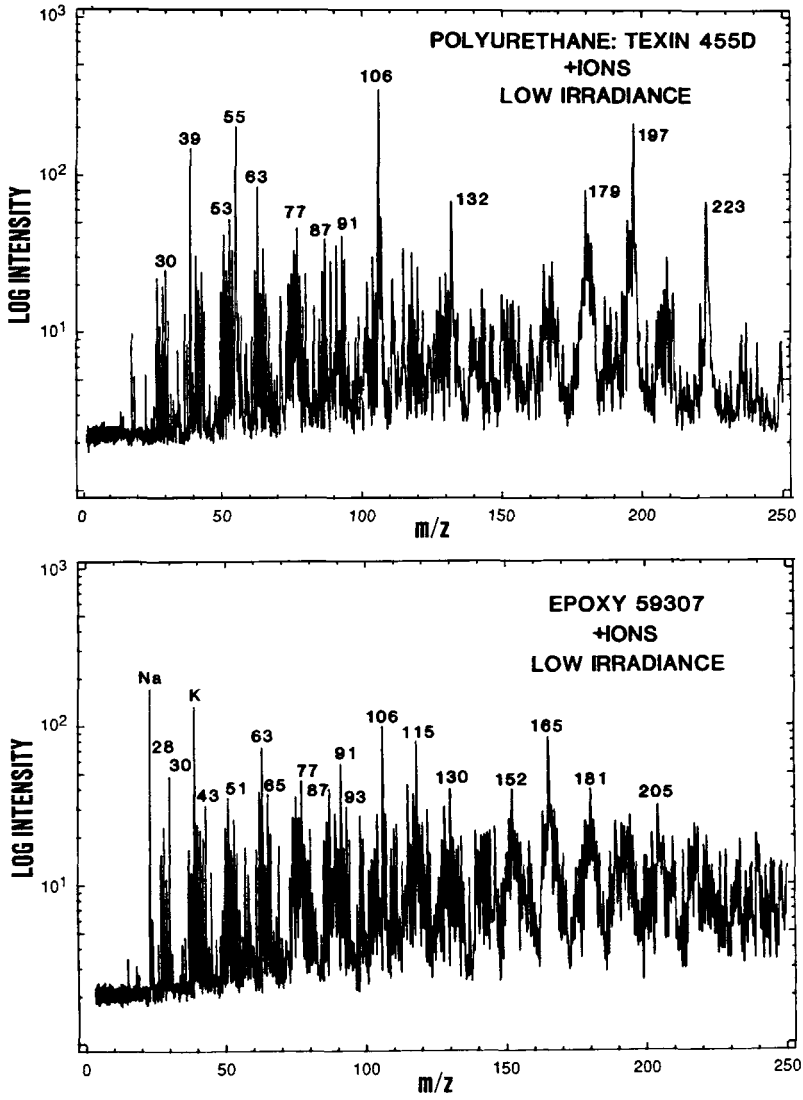

Fig. 2. Low-irradiance, positive ion LIMS mass spectra of polyurethane and one DDS/TGDDM epoxy.

The spectra in Figure 4 are examples of negative ion mass spectra produced from the photoresist and one of the polyimide samples. The negative ion spectra generally contain intense C_x^- ion signals in contrast to the more intense $C_xH_y^+$ cluster ions observed in the positive ion analyses.[15] These two spectra are quite similar except for the high-intensity m/z 26 (CN^-) ions detected in the polyimide spectrum.

The influence of laser irradiance variations on positive ion production and a comparison of positive and negative spectra for Mylar 500D are summarized in Figure 5. The major effect of a change in laser power results in both the number and intensity of the observed peaks. The high-intensity spectrum [Fig.

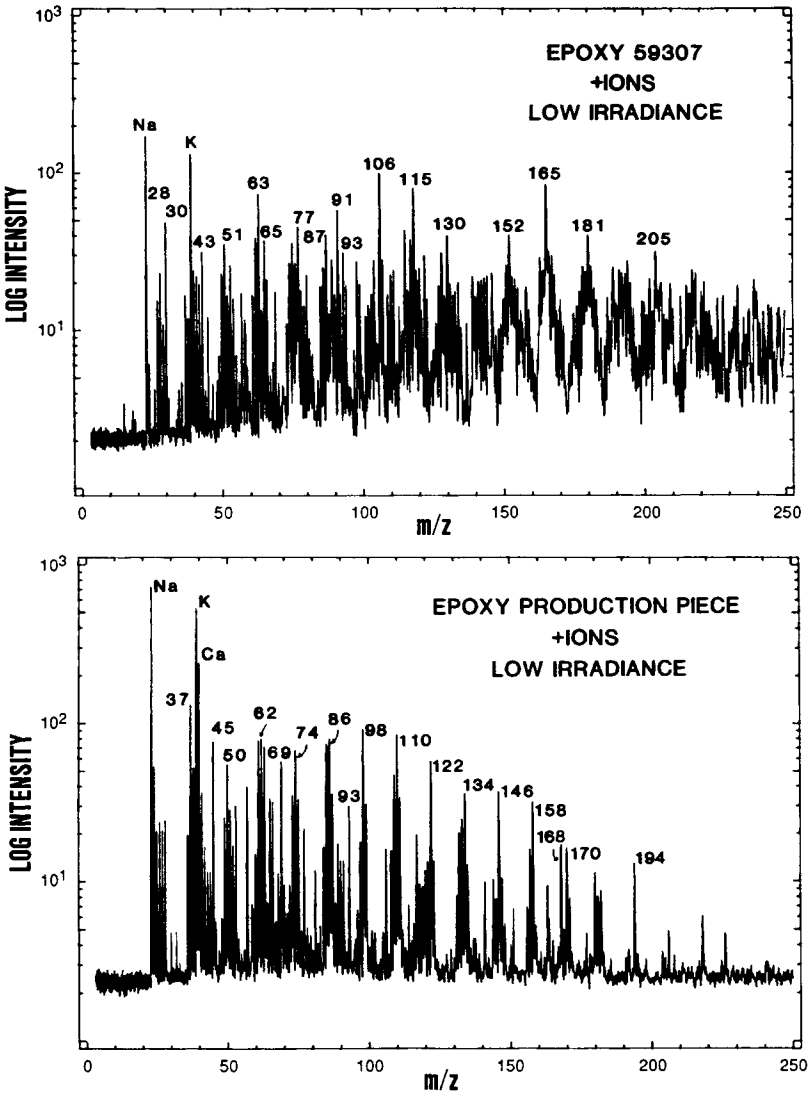

Fig. 3. Low-irradiance, positive ion LIMS mass spectra of two DDS/TGDDM epoxies.

5(a)] when compared to the medium- and low-intensity spectra [Fig. 5(b) and (c)] shows a systematic decrease in the number of peaks and their respective ratios. The best reproducibility was obtained for the low irradiation energies. As expected, the low-irradiance negative ion spectrum in Figure 5(d) is quite different than its corresponding positive ion spectrum. An increase in power also caused an increase in peak intensities and in the total number of peaks. In contrast to the positive ion spectra, the best reproducibility for the negative ion work was obtained for the high-irradiance experiments.

There are several methods of analyzing the LIMS polymer data to determine the uniqueness of the mass spectra produced from different polymers. A qual-

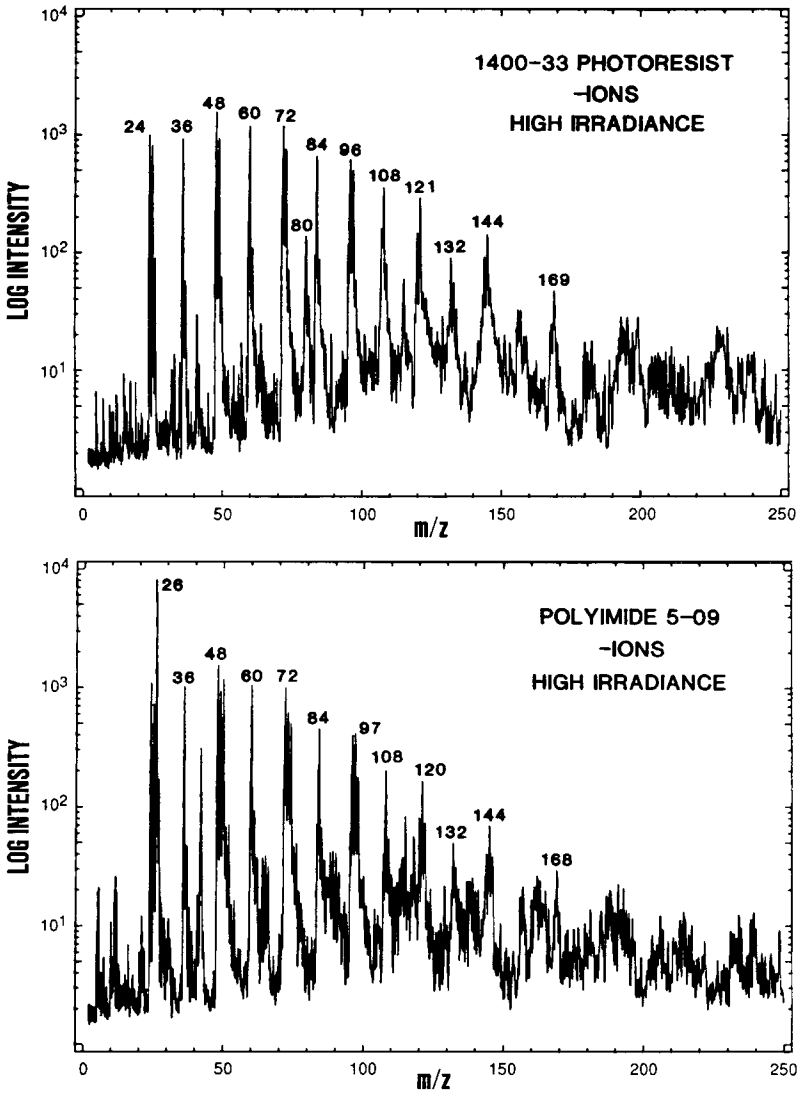

Fig. 4. High-irradiance, negative ion LIMS mass spectra of photoresist and polyimide samples.

itative comparison of the mass spectra shows the obvious high relative intensity of various $C_xH_y^+$ cluster ions. The distribution of these intensities for the various samples is not sufficiently unique to permit accurate classification of the polymer type. It is interesting to note, however, that the reproducibility of the various high-intensity ion signals produced for a given sample under a given analysis condition is quite good. The measured relative standard deviations of the peak area ion intensities for the more intense ion signals vary from 1 to 15% depending on the laser irradiance and the polymer. In general, the ion signals that contain the most chemical information (i.e., monomeric or obvious structurally related fragment peaks or aromatic structures) have low relative intensities and, hence, greater imprecision than the more intense $C_xH_y^+$ cluster ions.

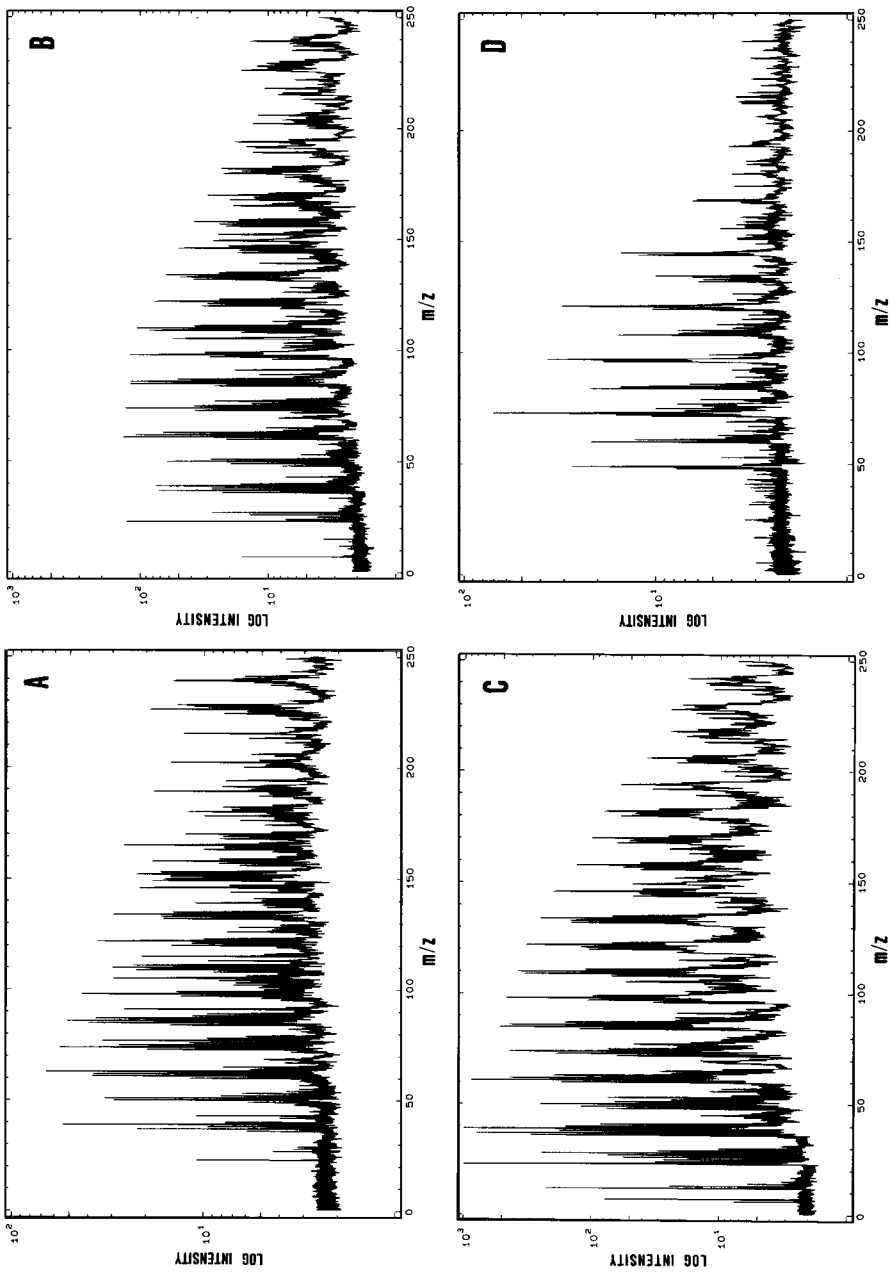

Fig. 5. A comparison of different irradiances and types of spectra for Mylar 500D: (a) low-irradiance, positive ion spectrum, (b) medium-irradiance positive ion, (c) high-irradiance positive ion spectrum, and (d) low-irradiance negative ion spectrum.

Since the qualitative comparisons of these various mass spectra are not sufficiently different to permit classification, the spectral data base was analyzed using pattern recognition techniques in order to determine whether the spectra from different polymers were in fact distinct.

The pattern recognition procedures employed in this study were based on principal component analysis/discriminant analysis techniques that employ the basic assumption that the data can be described by a linear combination of various factors (in this case, ion masses) having different weights or loadings.[16] The first step in all of the several commonly utilized factor analysis/discriminant analysis procedures is to determine the primary factors or principal components that best describe the data set.[17] Principal components were calculated by the power method.[18] Each principal component is a linear combination of the mass spectra in the data set. Spectra composed of principal components are referred to as factor spectra.

Once the principal components have been determined, discriminant analysis techniques can be performed on the mass spectral scores. Prior to discriminant analysis the polymers are categorized by their chemical composition. Discriminant analysis maximizes the variance among the average scores of the categories while minimizing the variance within each category.[10] The discriminant analysis procedure further reduces dimensionality of the spectra to $n - 1$ where n is the number of different categories. The orthogonal components obtained from discriminant analysis are referred to as the canonical variates. If the number of statistically significant canonical variates is less than $n - 1$, then the different categories will not be adequately resolved. In other words, some of the categories may be overlapped. The original data set can then be employed to cross validate the canonical variates.

The ability of the principal component analysis/discriminant techniques to qualitatively separate the various mass spectra into classes can be observed by plotting the scores. The relationships that exist among the mass spectra may be visualized, by examining the scores plotted on two components at a time.

Figures 6 through 10 illustrate component scores for the first two canonical variates observed in various analyses of the different polymer sets. The variance accounted for by the canonical variates is ranked from highest (first component) to the lowest (last component), and the largest contribution to the total variance is generally contained in the first few components. Figure 6 plots the scores for these two components obtained in the analysis of the high-irradiance, positive ion data produced from the first 7 polymers listed to Table I. This data set is comprised of 15 mass spectra (observations) for each polymer and the component score plot indicates good separation between the various classes of polymers as well as reasonably good (tight) clustering of the spectra in each class. Thus, the discriminant analysis technique qualitatively separates the spectra of the different polymers. A more quantitative measure of the uniqueness of these spectra is the accuracy of the cross validation analysis. Cross validation of the discriminant analysis results accurately classified 85% of the mass spectra while the expert system accurately classified 95% of the data for this high-irradiance, positive ion data set. These classification accuracies are quite good for this group of polymers.

Figure 7 plots the scores for the first 2 canonical variates for the data set of 5 randomly selected mass spectra obtained under high laser irradiance condi-

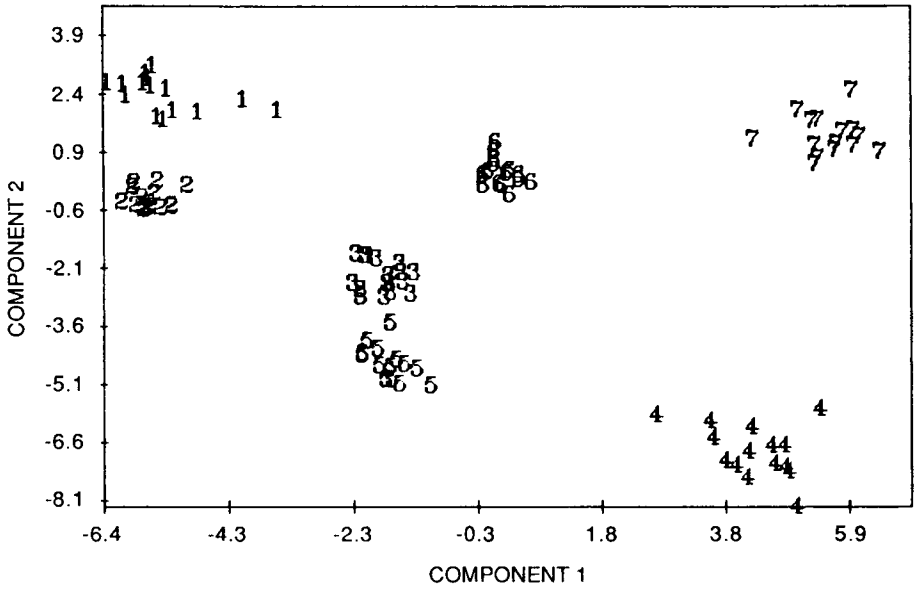

Fig. 6. Component score plot for first two linear discriminants for a data set comprised of high-irradiance, positive ion LIMS mass spectra of seven polymers. The polymers are identified by the following legend: (1) Nylon 6, (2) nylon 12, (3) poly(1,4-butylene) terephthalate, (4) polycarbonate, (5) polystyrene, (6) Spurrs epoxy, (7) Mylar 500D poly(ethylene) terephthalate.

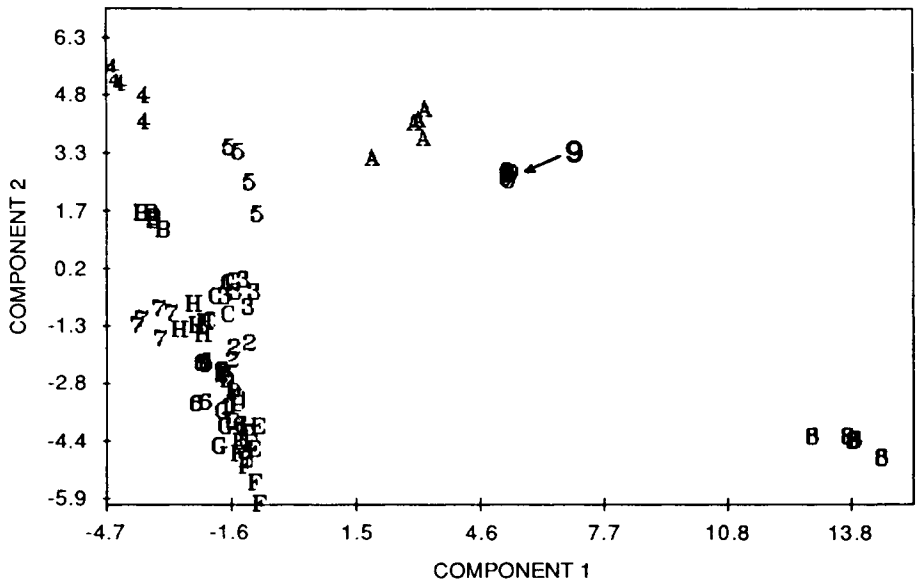

Fig. 7. Component score plot for first two linear discriminants for a data set comprised of high-irradiance, positive ion LIMS mass spectra of 17 polymers. The polymers are identified by the following legend: (1) Nylon 6, (2) nylon 12, (3) poly(1,4-butylene) terephthalate, (4) polycarbonate, (5) polystyrene, (6) Spurrs epoxy, (7) Mylar 500D, (8) polyimide S-09, (9) polyimide S-24: (A) Polyimide S-19, (B) photoresist 1400-33, (C) 59301 epoxy, (D) 59304 epoxy, (E) 59307 epoxy, (F) production epoxy, (G) 59306 epoxy, (H) Texin 455D.

tions from a group of 17 polymers. This more limited data set (i.e., the number of observations divided by the number of categories is smaller) does not exhibit a good separation. The software was able to process approximately 105 mass spectra at a time. The component score plot in Figure 7 does, however, illustrate good separation and clustering of the polyimide group (3 types), the photoresist and the polycarbonate. It is interesting to note that the poly(1,4-butylene) terephthalate and polycarbonate spectral data separate reasonably well in this data set. The canonical variate classification accuracy for this group of polymers is only 39%, which reflects the limited number of observations in this data set. The expert system accurately classified 60% of this data.

Figure 8 plots the component scores for the first 2 canonical variates from a low-irradiance, positive ion analysis of the full set of 19 polymers. Five mass spectra were randomly selected for each polymer. Several of the polymers separated reasonably well including the polyurethane, polyimides, one of the DDS/TGDDM formulations, and nylon 6. The cross validation accuracy for this set of data was 36% while the expert system classification yielded a cross validation accuracy of 63%.

The next two component score plots represent sample groups that are increasingly difficult to distinguish mass spectrometrically. As previously discussed, the spectra from these two polymer types were very similar. Figure 9 is a plot of the component scores for the first two canonical variates obtained from a data set comprised of a high-irradiance, negative ion spectra produced

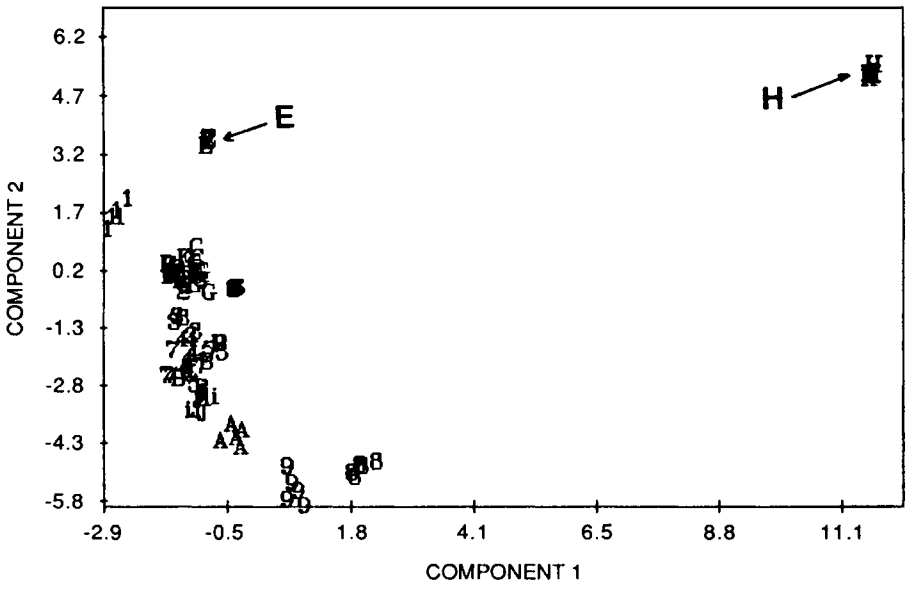

Fig. 8. Component score plot for the first two linear discriminants for a data set comprised of low-irradiance, positive ion LIMS mass spectra of 19 polymers. The polymers are identified by the following legend: (1) Nylon 6, (2) nylon 12, (3) poly(1,4 butylene) terephthalate, (4) polycarbonate, (5) polystyrene, (6) Spurrs epoxy, (7) Mylar 500D, (8) polyimide S-09, (9) polyimide S-24: (A) Polyimide S-19, (B) photoresist 1400-33, (C) 59301 epoxy, (D) 59304 epoxy, (E) photoresist, (F) production epoxy, (G) 59306 epoxy, (H) Texin 455D, (I) polyimide S-11, (J) polyimide S-10.

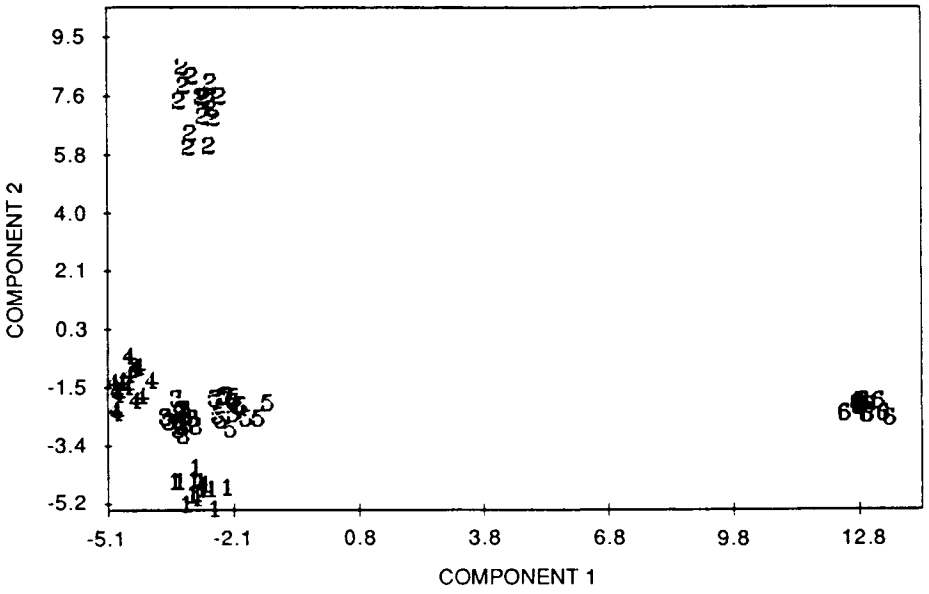

Fig. 9. Component score plot for the first two linear discriminants for a data set comprised of high-irradiance, negative ion LIMS mass spectra of five polyimide and one photoresist sample. The polymers are identified by the following legend: (1) Polyimide S-11, (2) polyimide S-09, (3) polyimide S-24, (4) polyimide S-10, (5) polyimide S-19, (6) photoresist 1400-33.

from the polyimide and photoresist samples. This data shows that the structure of the five polyimides are similar to each other but different from the photoresist material. The pattern recognition results are clearly more conclusive than the visual inspection of the spectra. Pattern recognition has been demonstrated to provide differentiation capabilities in many cases where differences among peaks in a set of mass spectra might be as subtle as intensity changes in only two or three peaks.

The photoresist spectra (group 6) are readily distinguished from the various polyimides, and there is good separation of the group 1 and 2 polyimides. The canonical variate cross validation yielded a classification accuracy of 60% while the expert system correctly classified 75% of the spectra. The analysis and classification of the spectra of polyimides and photoresist has very important applications in the microelectronics industry in which it is often necessary to determine the composition of suspected organic residues of these types of compounds on Si or GaAs substrates. These residues can adversely affect the performance of semiconductor devices and are present on the substrate surfaces because of incomplete photoresist removal and/or misalignments in the various masking steps. These residues typically have micrometer or submicrometer dimensions, and thus an organic microprobe technique is required for their identification. The component scores illustrated in Figure 9 indicate that the principal component/discriminant technique can provide a useful method for distinguishing these different compounds within micrometer diameter areas.

The component scores illustrated in Figure 10 represent an even more difficult analytical problem. The data set for this analysis was the low-irradiance, positive ion mass spectra produced from various DDS/TGDDM epoxy compositions.

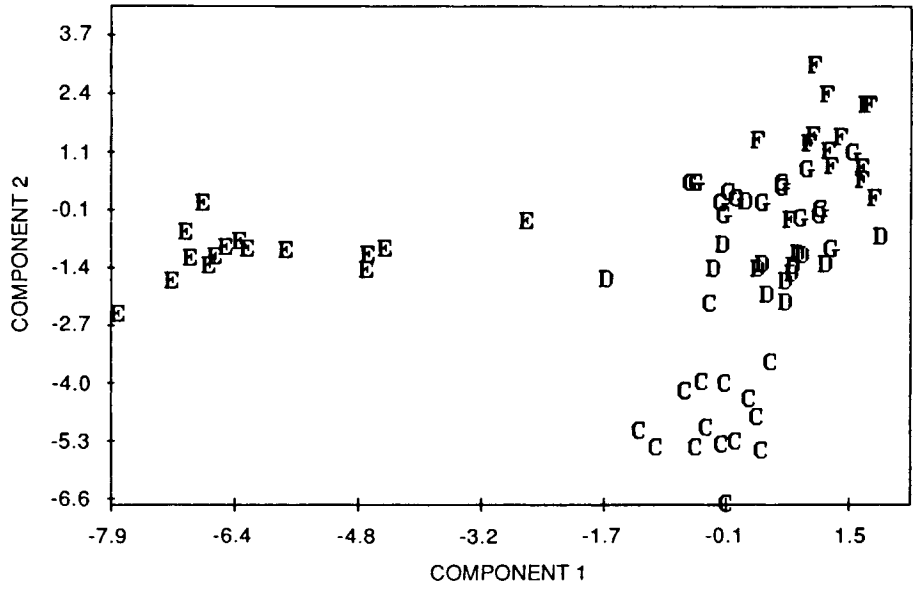

Fig. 10. Component score plot for the first two canonical variates for a data set comprised of low-irradiance, positive ion LIMS mass spectra of the five DDS/TGDDM epoxy formulations. The polymers are identified by the following legend: (C) 59301 Epoxy (0.2), (D) 59304 epoxy (0.75), (E) 59307 epoxy (1.5), (F) production epoxy, (G) 59306 epoxy (1.0).

These compositions differed in the gram equivalent amount of DDS hardener added to the bulk TGDDM/Novolac resin mixture. It is well known that the physical properties of the DDS/TGDDM epoxy including its ability to strongly bond continuous carbon fibers are very dependent on the DDS/TGDDM mixture ratios.[19] One problem associated with using this epoxy system as a carbon fiber reinforcement matrix is that although optimum bulk DDS/TGDDM mix ratios of 0.75–0.85 can be prepared, the bulk resin/hardener blend can segregate about the micrometer diameter carbon fibers producing poor fiber/matrix bonding. This inadequate bonding can result in delamination of the fibers from the matrix that could produce catastrophic consequences in the use of this carbon fiber/epoxy system for such applications as aerospace components. Thus, the ability to determine the DDS/TGDDM ratios at the actual fiber/matrix interface coupled with a knowledge of the bulk hardener/resin ratios and the macroscopic physical properties of the fiber/matrix system could provide a method for certifying the optimum DDS/TGDDM blend ratios required for adequate bonding. The component score plot in Fig. 10 illustrates that the production epoxy formulation that represents a blend ratio having good bonding characteristics can be separated from both the C and E samples. The ratio of DDS to TGDDM for the production epoxy equals 0.8 (the gram equivalent weight ratios are given in parenthesis in the legend of this plot) while the C samples have low (0.2) DDS/TGDDM ratios and the E samples have high (1.5) hardener to resin ratios. Thus, the discriminant analysis technique separates the extreme DDS/TGDDM ratios; however, it does not adequately separate the resin/hardener ratios, which are quite similar. The cross validation classification accuracy of the discriminant analysis and the expert system for

this data set was 60%. Although this classification accuracy is not adequate for rigorous quality control analysis of these epoxy formulations, the technique of partial least-squares regression analysis[20] could possibly provide a much higher accuracy for the classification of the spectra from this chemically complex system.

CONCLUSIONS

The principal component analysis techniques suggest that the optimum classification accuracy for LIMS spectra of polymeric materials is on the order of 80%. This level of predictive accuracy is sufficient for a number of applications requiring a qualitative identification of the presence or absence of an organic polymer on various substrates. Improvements in the accuracy can possibly be achieved by increasing the data base size and/or by preclassifying spectra with respect to polymer type. This preclassification procedure might involve developing discriminant analysis data bases of selected polymer groups such as aromatic and nonaromatic polymers, photoresists, and polyimides. Approaches to various types of preclassification are being explored. The use of partial least-squares regression techniques may find extensive utilization in quantitatively classifying different relative concentration levels in chemically similar polymers, and this classification technique is currently under evaluation.

The results of the polymer analysis by laser microprobe mass spectrometry demonstrate that the technique can provide useful, sensitive qualitative organic microanalysis of a wide range of chemical species. The utility of this technique for organic characterizations applied to a wide range of fundamental and practical analytical problems will depend on the development of mass spectral data bases, library search routines, as well as the implementation of pattern recognition software routines. These approaches will demand that acceptable intra- and interlaboratory reproducibility be established for the technique.

Charles Evans & Associates acknowledges support for this research from the National Science Foundation, Small Business Innovation Research Program, Grant #ISI-8760431.

References

1. R. Kaufmann and P. Wieser, in *Modern Methods of Fine Particle Characterization*, Vol. III, CRC Press, Boca Raton, FL, 1982.

2. H. Vogt, H. J. Heinen, S. Meier, and R. Wechsung, *Fres. Zeit. Anal. Chem.*, **308**, 195 (1980).

3. D. S. Simons, *Appl. Sur. Sci.*, **31**, 102 (1988).

4. See, for example, papers contained in the *Proc. Third Int'l Laser Microprobe Mass Spectrometry Workshop*, August 26–27, 1986, University of Antwerp, Antwerp, Belgium.

5. A. Z. Wilk and D. M. Hercules, *Anal. Chem.*, **59**, 1819 (1987).

6. D. E. Mattern and D. M. Hercules, *Anal. Chem.*, **57**, 2041 (1985).

7. L. V. Vaeck, J. Claereboudt, J. DeWaele, E. Esmans, and R. Gijbels, *Anal. Chem.*, **57**, 2944 (1985).

8. D. L. Massart, B. G. M. Vandeginste, S. N. Deming, Y. Michotte, and L. Kaufman, *Chemometrics: A Textbook*, Elsevier, New York, 1988.

9. P. B. Harrington, K. J. Voorhees, T. E. Street, F. R. di Brozolo, and R. W. Odom, *Anal. Chem.*, **61**, 715 (1989).

10. T. Dingle, B. W. Griffiths, J. C. Ruckman, and C. A. Evans, Jr., in *Microbeam Analysis*—1982, K. F. J. Heinrich, Ed., San Francisco Press, San Francisco, p. 385.

11. J. R. Quinlan, in *Machine Learning: An Artificial Intelligence Approach,* R. S. Michalski, J. G. Carbonell, and T. M. Mitchell, Eds.; Tioga Publishing, Palo Alto, CA, 1983.

12. P. B. Harrington and K. J. Voorhees, *Anal. Chem.,* **62,** 729 (1990).

13. R. J. Morgan, J. E. O'Neal, and D. B. Miller, *J. Mats. Sci.,* **14,** 109 (1979).

14. F. R. Di Brozolo, in *Secondary Ion Mass Spectrometry, SIMS VI,* A. Benninghoven, A. M. Huber, and H. W. Werner, Eds., Wiley, New York, 1988, p. 607.

15. K. Balasanmugan, S. K. Viswanadham, and D. M. Hercules, *Anal. Chem.,* **58,** 1102 (1986).

16. E. R. Malinowski and D. G. Howery, Eds., *Factor Analysis in Chemistry,* Wiley-Interscience, New York, 1980.

17. D. Child, Ed., *The Essentials of Factor Analysis,* Holt, Rinehart and Winston, New York, 1970.

18. G. Strang, Eds., *Linear Algebra and Its Applications,* Academic Press, New York, 1980.

19. H. S. Chu and J. C. Deferis, *Polymer Comps.,* **5,** 124 (1984).

20. P. Geladi and B. R. Kowalski, *Anal. Chem. Acta,* **185,** 1 (1986).

Received June 2, 1989
Accepted November 20, 1989